Sixth International Symposium on Turbulence and Shear Flow Phenomena
Seoul, Korea, 22-24 June 2009

ASYMMETRIES IN THE WAKE STRUCTURE OF A FORMULA 1 TIRE

John Axerio
Mechanical Engineering Department
Stanford University
Bldg. 500-RM500 H, Stanford, CA, USA, 94305-3035
axerio@stanford.edu

Gianluca Iaccarino
Mechanical Engineering Department,
Stanford University
Bldg. 500-RM500 I, Stanford, CA, USA, 94305-3035
gianluca.iaccarino@stanford.edu

ABSTRACT

The flow field around a 60% scale stationary and rotating Formula 1 tire was examined both experimentally and computationally in order to investigate the complex near wake flow field. The results of steady RANS simulations were compared to PIV data at two cross flow planes downstream of the tire in order to validate the numerical predictions and to confirm the existence of large scale flow features. Four different tire configurations were tested in order to understand how the wake structure was influenced by various geometrical features. The protruding upper main rotor duct, lower fin caliper duct, wheel camber angle, outboard hub cavity, and airflow through the hub all create asymmetries in the wake of the tire. It is shown that out of all the aforementioned geometrical features, the most critical is the flow through the hub. Simplifying the computational mesh by removing inner brake components (caliper, covers, bearings, rotor, electronics) changes the net positive mass flow through the outboard spokes, and consequently changes the intensity and location of the two main counterrotating vortices in the far wake region.

INTRODUCTION

The purpose of this paper is to identify the main flow features behind stationary and rotating Formula 1 tires, and try to answer questions about how these structures are created, convected, and eventually destroyed. There have been many studies that address isolated stationary and rotating wheels, but only a few recently have addressed the issue of generating a simplified model for the complex near wake structure. Many investigations have compared pressure contours around the surface of the tire to determine lift and drag forces, as well as characterized the behavior of various turbulence models. This paper will focus more on characterizing the asymmetries associated with the flow around a true Formula 1 tire and hub geometry.

The work of Fackrell et al. (1973), Morelli (1969), and Stapleford et al. (1969) serve as the foundation upon which further details of the complex wake structure were revealed. McManus et al. (2006) identified regions of separated flow, counterrotating vortices, and arch shaped vortices, which are all fundamental features related to isolated tire aerodynamics. Only recently has there been experimental evidence backing up a proposed model by Saddington et al. (2007) of the trailing vortex system of an isolated wheel rotating in contact with the ground. This model proposes that there is a region of velocity deficit behind the tire in the shape of an inverted-T. This region is dominated by a large pocket of reversed flow that extends beyond the tire projected profile. A trailing vortex system consisting of two counterrotating vortex pairs is also present. The stronger of the two pairs is near the ground plane, while the weaker pair is closer towards the top of the tire. The strong ground vortex pair has its cores aligned with the edge of the tire shoulder, and does not spread laterally until one wheel diameter downstream from the wheel axis. The upper vortex pair is not as large or intense as the ground pair, and as a result the upper pair merges with the ground pair within one wheel diameter downstream.

Knowles (2005) provided an explanation for the reversed flow regions outside the projected profile of the tire. He explains that it is due to the impingement of the flow at the front of the contact patch which produces two strong lateral jets. These jets widen the effective tire profile, and as a result create a wider wake of reversed flow. Knowles was one of the first authors to perform experiments and simulations of a Formula 1 tire hub that allowed air to flow through the tire hub. A majority of his work was focused on characterizing the influence of the support sting on the wake of the tire. A key conclusion was that the support sting increased the mass flow through the spokes by almost 60%, entraining flow into the formation region of the upper vortex pair. The end result was the attenuation of the upper vortex. Overall though, the sting did not create strong asymmetry behind the tire, and had little impact on the overall shape and extent of the wake.

The work of Knowles (2005) contradicts some of the conclusions made by Nigbur (1999) in which he explains possible reasons for the asymmetrical wake structure for a rotating isolated wheel. The three reasons given for the very asymmetric wake were the support sting, the asymmetric hub geometry, and the placement of the wheel in the tunnel (the tire was not centered on the moving belt). It will be shown in this paper that the primary reason for this asymmetry is not any of these reasons, rather it is the flow through the tire. The asymmetric hub geometry causes a difference in pressure between the inboard and outboard sides of the tire, and therefore drives flow through the inside of the hub. It is this flow that creates the asymmetry, not the geometry.

DESCRIPTION OF TIRE GEOMETRY AND SETUP

Two different wheel geometries were tested experimentally and are shown in figure 1 and figure 2. In all configurations tested, the 60% scale front right tire of the race car was chosen and placed in the middle of the wind tunnel. The tire is held in place by a support sting shrouded with a symmetric airfoil. The sting is attached to the outboard side of the tire and should not be confused with the suspension arms in a real vehicle setting. For the stationary tests, all walls are fixed. For the rotating tests, a rolling road system is used in order to simulate the moving ground and tire. The Reynolds number based on the wheel diameter and inlet velocity is 5.0e5. Figure 1 shows the front and rear isometric views of the Formula 1 tire with wheel fairings on both the inboard and outboard sides of the hub (configuration I). Formula 1 teams are now experimenting with different wheel fairings on the outboard side of the hub. Figure 2 (configuration II) shows the true Formula 1 tire with all interior components (caliper, rotor, bearings, covers) and exterior components (upper main rotor duct, lower fin caliper duct).

(a) Inboard Front View (b) Outboard Rear View

Figure 1: Simplified wheel geometry with wheel fairings on both sides of rim - Configuration I

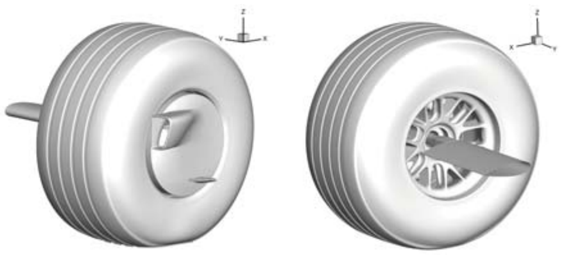

(a) Inboard Front View (b) Outboard Rear View

Figure 2: Full wheel geometry with ducts, passages, and brake assembly - Configuration II

The tire geometries for all cases shown in this paper are tilted inwards at 2.5° such that the top of the tire is closer to the car centerline. Different camber angles were tested (specifically 2.5° and 3.25°) both experimentally and computationally, and it was shown that although the location of vortex cores change slightly, qualitatively the wake remains unchanged.

Four different wheel geometries were simulated using a RANS solver. In addition to the two wheel configurations (I and II) previously mentioned, two additional configurations were simulated in order to verify key conclusions. Figure 3 (configuration III) is similar to configuration II, but all passages through the hub are blocked. This configuration confirms the influence of flow through the hub when compared to configuration II. Configuration IV (not shown) is geometrically identical to configuration I, but a mass flux is imposed through a small section of the full fairing (circular segment) such that flow exits 20° outwards from the fairing face and angled 45° downwards from the horizontal plane. The circular segment is defined such that the chord bisector is angled 45° down from the horizontal (downstream lower half of fairing), and the area of the segment is 20% the size of the full outboard fairing.

In all rotating simulations, the fairings and brake ducts do not rotate. The only rotating components are the rubber wheel surface, hub, and rotor. The influence of the rotating components was investigated by applying a multiple reference frame (MRF) model to the volume of air inside the rotor, as well as the volume of air inside the spokes (Luo et al. (1994)). The results show that when rotating MRF's are used, the wake behind the tire is smaller. It was shown by Bienz et al. (2003) that the proper treatment of rotating volumes is essential when performing rotating wheel simulations. They show that applying a rotating boundary condition to only the walls is insufficient in capturing the behavior of air flow through rotating volumes.

The specifics regarding the experimental PIV (particle image velocimetry) setup, as well as the computational mesh details, RANS solver and boundary conditions are described in the work by Axerio et al. (2009). The mesh size that was used for the full brake duct geometry was approximately 30 million cells. The specific RANS turbulence model used for all simulations in this paper is the SST k-ω model by Menter (2003).

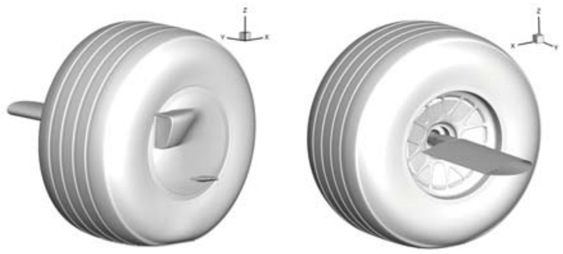

(a) Inboard Front View (b) Outboard Rear View

Figure 3: Simplified wheel geometry with exterior brake ducts and spokes, but all passages are blocked - Configuration III

RESULTS AND DISCUSSION

The results given in this paper are presented in two sections. The first section concerns the stationary tire, while the second section describes rotating tires. The reason for studying both operating conditions is to determine the sensitivity in the wake asymmetry to large scale separation. A stationary tire's wake is much smaller than a rotating tire. A stationary tire is similar to a finite span cylinder. It is well known that the flow around a cylinder with infinite span separates immediately behind the cylinder. A finite span cylinder does not have such a large wake. This is due to the side flow transferring energy to the top flow, casing the entrainment of flow from the top of the tire downwards. This downwards movement creates a strong downwash region which fuels the formation of the strong counterrotating ground vortex pair (CVP).

Stationary

Figure 4(a) shows the wake immediately behind the stationary configuration I tire. The velocity field is very symmetric about the wheel center plane. The presence of the ground counterrotating vortices is particularly evident, and the two ground lobes project past the wheel profile. It is very clear from the full 3D flow field that the ground vortex pair begins at the front of the contact patch due to the jetting caused by the impingement of the tire and stationary ground.

One feature that is revealed from the simulations that has not been documented in the past literature is the presence of weak vortices (labeled ‘C’ and ‘D’ in figure 4(a)) that are generated from the tire shoulders near the aft of the tire (back of the tire). These vortices should not be confused with the ‘hub’ vortices (vortices created by the hub cavity) that are mentioned in the work of Cogotti (1983) and Mercker et al. (1992). The evidence presented in this paper as well as the work of Saddington et al. (2007) disputes the existence of ‘hub’ vortices.

The vortices are not generated at the hub (configuration I uses ‘hub’ covers), but rather a result of the low pressure region immediately below the aft of the tire and create wing tip-like vortices that shed from the tire shoulder. In the rotating simulations these vortices are much higher from the ground plane (near the top of the tire) and have been well documented in the past. These vortices are much weaker than the strong ground vortices, and as a result, at x/D=0.75 the upper vortex pair is no longer present. A particle in the core of these weak vortices will actually propagate upstream due to the negative x-velocity.

Figures 4(b) and 4(c) show in-plane velocity vectors for two different downstream planes. Even though the wheel is cambered and has a support sting, the trailing vortex pair is very symmetric about the wheel center plane.

The primary importance for the stationary case is to highlight the differences between configurations I and II. The first difference when looking at figure 5(a) is the larger size of the outboard (right) vortex. The downwash region is still strong, but not as strong as configuration I. Also, the downwash moves from right to left due mainly to the camber and support sting. Moving downstream (5(b) and 5(c)) the downwash moves from left to right. This is due to the much stronger cross flow shown by the arrow labeled ‘E’ in figure 5(a). The reason why there is a much stronger cross flow on the inboard side compared to the outboard side of the tire is due to the air moving from left to right through the tire. Also, the main brake duct on the inboard side sucks in a substantial amount of air. This creates a low pressure region behind the duct, which strengthens the cross flow. The flow that exits near the top of the outboard hub immediately gets entrained towards the top of the tire, creating a very strong asymmetric recirculation (at x/D=0.25) which eventually evolves into vortex ‘D’ in figure 5(c). The end result is that vortex ‘A’ in figure 5(c) completely dominates the wake as well as vortex ‘B’ (vortex pair ‘A’ and ‘B’ form the CVP) due to the asymmetric downwash.

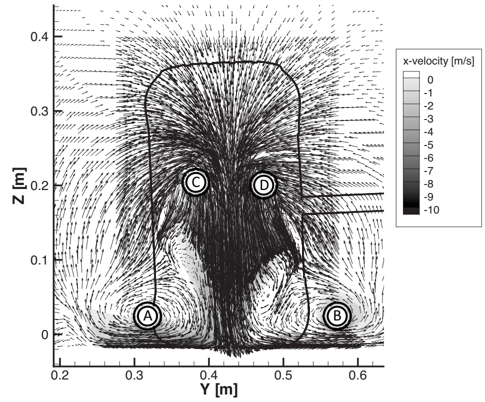

(a) CFD Plane x/D=0.51

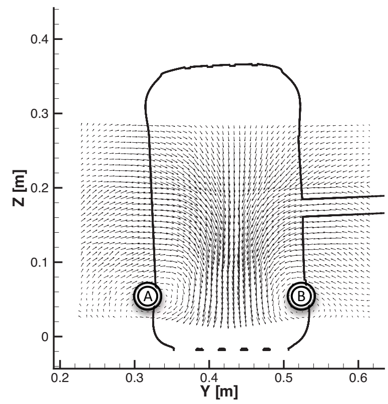

(b) Experiment Plane x/D=1.09

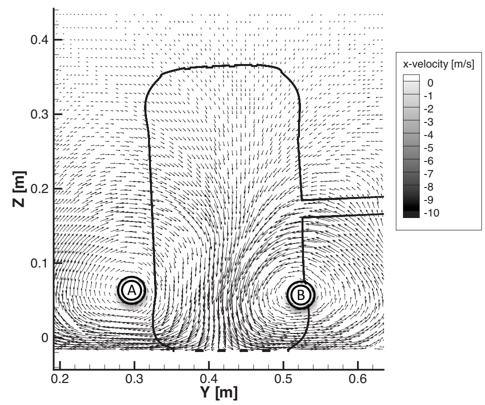

(c) CFD Plane x/D=1.40

Figure 4: Simplified Stationary Tire with Fairings (I)

Rotating

The key difference between the rotating wake structure and the stationary wake structure is that the rotating wake structure is much narrower and taller than the stationary wake. The downwash and CVP are not as strong, but the recirculation region in the wake of the rotating tire is much larger. A particle 1.5 wheel diameters downstream from the wheel axis will spin slowly upstream until it reaches the rear of the contact patch. It then convects towards either the inboard or outboard sides of the tire, then accelerates as it gets entrained by the shear layer. The shear layer is caused by the lateral jets formed at the front of the contact patch by the impingement of the ground and tire. Vortices ‘C’ and ‘D’ mentioned in the previous section are much more evident

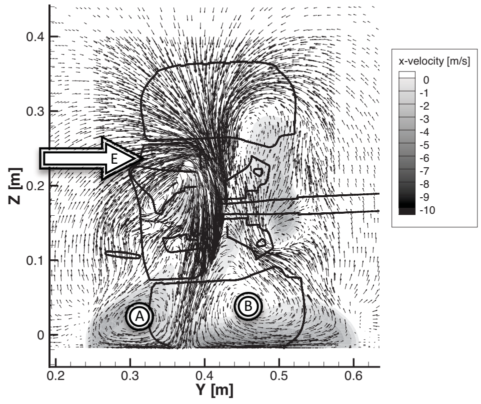

(a) CFD Plane x/D=0.51

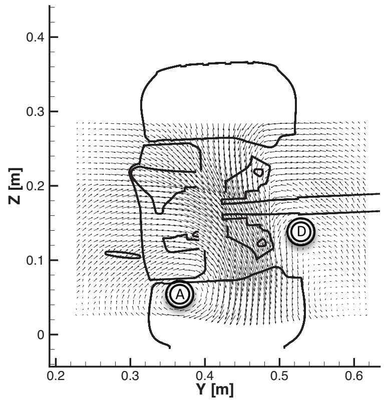

(b) Experiment Plane x/D=1.09

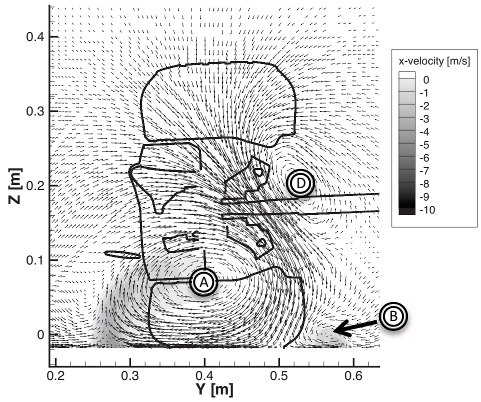

(c) CFD Plane x/D=1.09

Figure 5: Stationary Tire with Full Brake Assembly (II)

for a rotating tire. Since separation occurs at the top of the tire, these vortices are formed from the tire shoulder at the top of the tire (as opposed to the back of the tire for the stationary case).

In the literature there is no information regarding the direction of propagation of a particle inside any of these vortex pairs. A particle released in the the uppper vortex will actually propagate upstream until it hits the shear layer at the top of the tire. It then shoots downstream and does not interact with the ground CVP until very far downstream.

Figure 6(a) shows the rotating simplified tire with fairings. The vector field is very symmetric, and the presence of the upper vortex pair ('C' and 'D') is evident. The two arrows in this figure show the flow trying to fill the area right behind the tire due to the low pressure caused by the strong separation bubble. The arrows eventually converge downstream and form the beginning of the downwash region.

Figure 6(b) shows the asymmetry in the wake caused by the wheel camber and support sting. The outboard vortex is larger than the inboard vortex and the downwash region moves slightly from right to left. Even though the wake in this plane is not symmetric, it is still easy to discern which vortices correspond to the ground CVP. The same conclusions can be said about figure 7. Despite the geometry being strongly asymmetric, the ground CVP are extremely symmetric in figure 7(b).

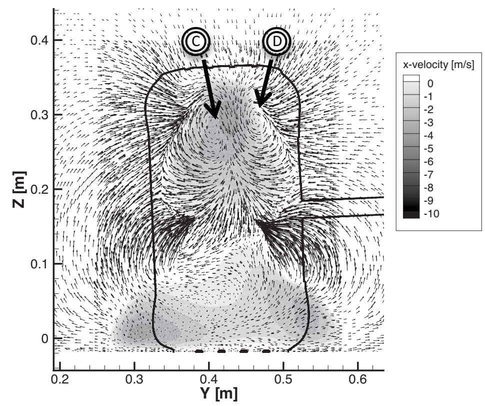

(a) CFD Plane x/D=0.51

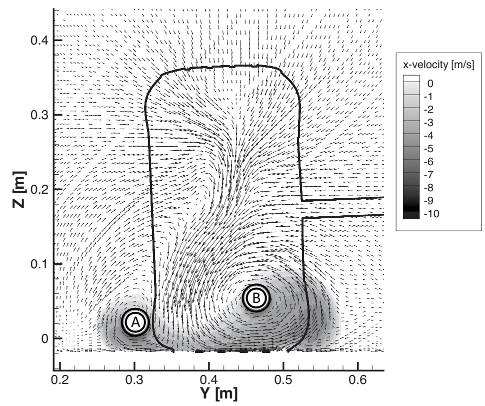

(b) CFD Plane x/D=1.09

Figure 6: Simplified Rotating Tire with Fairings (I)

Configuration II in figure 8 shows both the experimental and CFD planes at x/D=0.51 and x/D=1.09. The k-ω turbulence model matches very well with the experiments. Vortices 'C' and 'D' in 8(b) are in the same position and of the same intensity as the experiment. The right vortex of the ground CVP is completely overwhelmed by the left vortex, and the downwash region snakes from the top of the tire

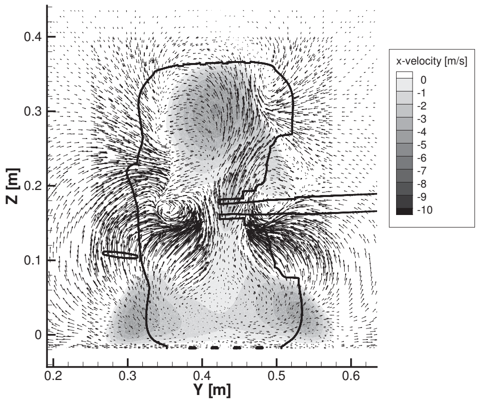

(a) CFD Plane x/D=0.51

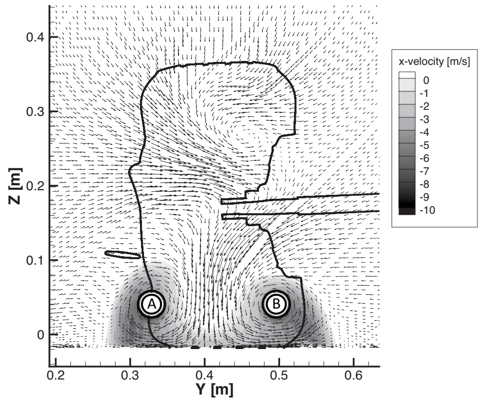

(b) CFD Plane x/D=1.09

Figure 7: Simplified Rotating Tire with Exterior Ducts (III)

towards the outboard side, and then back towards the center plane of the tire. It is evident from figures 8(c) and 8(d) that the upper vortex 'C' is no longer present. The lower wake is dominated by the strong inboard ground vortex. Vortex 'D' in this figure should not be misrepresented as one of the vortices in the ground CVP. This vortex is the outboard vortex in the top CVP that does not dissipate downstream. The reason why the inboard vortex dissipates for the top CVP is due to the strong cross flow (labeled 'F' in figure 8(b)). The reason why there is no strong cross flow from the outboard side of the tire towards the center is because the flow through the hub collides head on with the cross flow, essentially canceling out all the in-plane momentum in that region.

In order to verify the proposition that a majority of the wake asymmetry is caused by the flow through the tire, a hypothetical test case was simulated. The mass flow rate through the hub was extracted from the rotating configuration II geometry and the same mass flow rate was imposed on a small section of the outboard fairing of the configuration I geometry. The results of this simulation are shown in figure 9. The cross flow of the inboard side of the wheel in 9(a) is much stronger than the outboard side, and the mass flow coming out of the outboard fairing feeds the downwash region causing it to move from right to left. As the flow moves downstream, the downwash fuels the inboard ground vortex, while annihilating the outboard ground vortex.

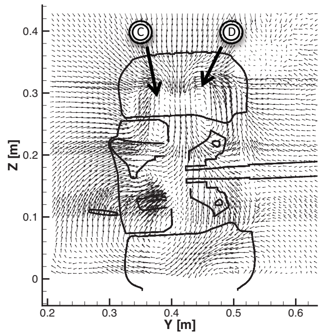

(a) Experiment Plane x/D=0.51

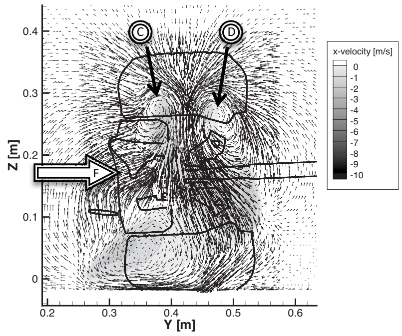

(b) CFD Plane x/D=0.51

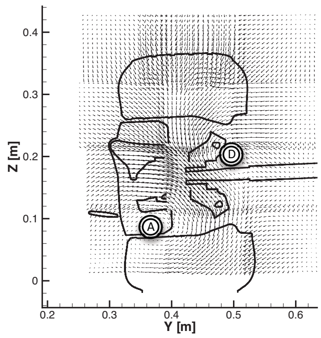

(c) Experiment Plane x/D=1.09

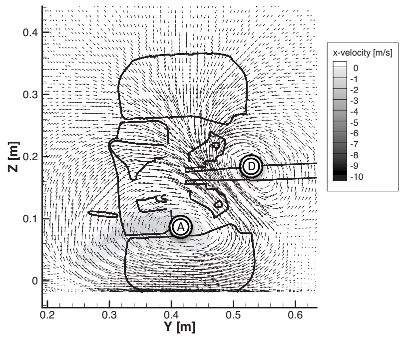

(d) CFD Plane x/D=1.09

Figure 8: Rotating Tire with Full Brake Assembly (II)

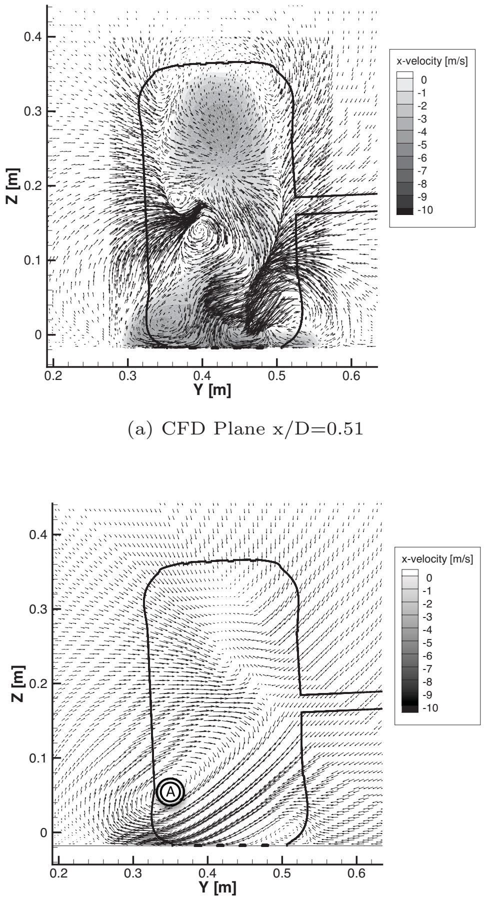

(a) CFD Plane x/D=0.51

(b) CFD Plane x/D=1.09

Figure 9: Simplified Rotating Tire with Exhausting Fairings (IV)

CONCLUSIONS

The primary reason for the velocity asymmetry in cross flow planes behind a 60% scale Formula 1 tire is shown to be caused by the flow through the hub of the tire. Four different tire configurations were tested both experimentally and computationally that provide very good evidence to support this claim. The flow field around a rotating Formula 1 tire is shown to be more susceptible to asymmetry compared to a stationary tire due in large part to the larger separation region. The flow field behind a tire with wheel fairings on both sides is quite symmetric despite the presence of a support sting. The counterrotating vortex pair that dominate the wake behind a geometrically symmetrical tire are no longer of the same intensity when the fairings are removed, and the flow is allowed to enter the hub. The flow that exits from the outboard face of the Formula 1 tire adds momentum to the strong downwash region immediately behind the tire, thus weakening the outboard vortex, and increasing the size and intensity of the inboard vortex.

ACKNOWLEDGEMENTS

The authors wish to thank John Eaton's experimental group at Stanford University, specifically Emin Issakhanian, Kin Lo, and Chris Elkins for providing the experimental data used for the comparisons in this paper. The authors also wish to thank Toyota Motor Corporation - F1 Motorsports Divsion for their financial support of this work.

REFERENCES

Axerio, J., Iaccarino, G., Issakhanian, E., Lo, K., Elkins, C., and Eaton, J., 2009, "Computational and Experimental Investigation of the Flow Structure and Vortex Dynamics in the Wake of a Formula 1 Tire", *Society of Automotive Engineers*, Warrendale, PA, 2009-01-0775.

Bienz, C., Larsson, T., Sato, T., and Ullbrand, B., 2003, "CFD at Sauber Petronas F1. Leading the Aerodynamics Development", *Proceedings of the 1st European Automotive CFD Conference*, Frankfurt, Germany.

Cogotti A., 1983, "Aerodynamic characteristics of car wheels", *Int. J. Vehicle Des. Technol. Adv. Vehicle Des. Ser. SP3, Impact of aerodynamics on vehicle design*, pp. 173-196.

Fackrell J. E., and Harvey, J. K., 1973, "The Flow Field and Pressure Distribution of an Isolated Road Wheel", *Advances in Road Vehicle Aerodynamics*, Paper 10, pp. 155-165, BHRA.

Knowles, R. D., 2005, *Monoposto racecar wheel aerodynamics: Investigation of near-wake structure and support sting interference*, Ph.D. Thesis, Cranfield University, Shrivenham, UK.

Luo, J. Y., Issa, R. I., and Gosman, A.D., 1994, "Prediction of Impeller-Induced Flows in Mixing Vessels Using Multiple Frames of Reference", *IChemE Symposium Series*, 136, pp. 549-556.

McManus J., and Zhang X., 2006, "A Computational Study of the Flow Around an Isolated Wheel in Contact With the Ground", *ASME J. Fluids Eng.*, 128, pp. 520-530.

Menter, F.R., 1993, "Zonal Two Equation k-ω Turbulence Models for Aerodynamic Flows", *AIAA* Paper 93-2906.

Mercker E., and Berneburg H., 1992, "On the simulation of road driving of a passenger car in a wind tunnel using a moving belt and rotating wheels", *Proceedings of 3rd international conference on innovation and reliability*, Florence, Italy.

Morelli A., 1969, "Aerodynamic Effects on an Automobile Wheel, Technical Report Translation 47/69, *MIRA*. Translated from Morelli, A., 1969, "Aerodynamic Effects on the Car Wheel", *ATA Review*, pp. 281-288.

Nigbur, J.E., 1999, *Characteristics of the Wake Downstream of an Isolated Automotive Wheel*, MSc Thesis, Cranfield University, Bedfordshire, UK.

Saddington A. J., Knowles R.D., and Knowles K., 2007, "Laser Doppler anemometry measurements in the near-wake of an isolated Formula One wheel", *Exp Fluids*, Volume 42, Number 5, pp. 671-681.

Stapleford W. R., and Carr, G. W., 1969, "Aerodynamic Characteristics of Exposed Rotating Wheels", Report No. 1970/2, *MIRA*, Nuneaton, U.K.